Paternal MHC expression on mouse trophoblast affects uterine vascularization and fetal growth

Zofia Madeja[a,b,1], Hakim Yadi[b,c], Richard Apps[b,d], Selma Boulenouar[b,e], Stephen J. Roper[a,b], Lucy Gardner[b,d], Ashley Moffett[b,d], Francesco Colucci[b,c,e,2], and Myriam Hemberger[a,b,2,3]

[a]Laboratory for Epigenetics, The Babraham Institute, Babraham Research Campus, Cambridge CB22 3AT, United Kingdom; [b]Centre for Trophoblast Research, University of Cambridge, Cambridge CB2 3EG, United Kingdom; [c]Laboratory for Lymphocyte Signaling and Development, The Babraham Institute, Babraham Research Campus, Cambridge CB22 3AT, United Kingdom; [d]Department of Pathology, University of Cambridge, Cambridge CB2 1QP, United Kingdom; and [e]Department of Obstetrics and Gynaecology, University of Cambridge Clinical School, and National Institute for Health Research Cambridge Comprehensive Biomedical Research Centre, Cambridge CB2 0SW, United Kingdom

Edited by R. Michael Roberts, University of Missouri, Columbia, MO, and approved January 14, 2011 (received for review April 20, 2010)

The mammalian fetus represents a semiallograft within the maternal uterus yet is not rejected. This situation is particularly pronounced in species with a hemochorial type of placentation, such as humans and rodents, where maternal tissues and blood are in direct contact with fetal trophoblast and thus potentially with paternal antigens. The main polymorphic antigens responsible for graft rejection are MHC antigens. In humans the trophoblast cells invading into the decidua have a unique pattern of MHC class I expression characterized by both classical (HLA-C) and nonclassical (HLA-G and HLA-E) molecules. Whether such an unusual MHC repertoire on the surface of trophoblast is a conserved feature between species with hemochorial placentation has not been resolved. Here we demonstrate, using a range of methods, that C57BL/6 mouse trophoblast predominantly expresses only one MHC class I antigen, H2-K, at the cell surface of giant cells but lacks expression of nonclassical MHC molecules. Antigenic disparity between parental MHCs affects trophoblast-induced transformation of the uterine vasculature and, consequently, placental and fetal gowth. Maternal uterine blood vessels were more dilated, allowing for increased blood supply, in certain combinations of maternal and paternal MHC haplotypes, and these allogeneic fetuses and placentas were heavier at term compared with syngeneic controls. Thus, maternal–fetal immune interactions are instrumental to optimize reproductive success. This cross-talk has important implications for human disorders of pregnancy, such as preeclampsia and fetal growth restriction.

decidual artery remodeling | uterine natural killer cells

Intrauterine development in viviparous mammals is an immunological paradox because the conceptus expresses paternal MHC transplantation antigens, yet it is not rejected (1, 2). This situation is particularly evident in hemochorial placentation (found in humans and mice), where fetal trophoblast cells penetrate deeply into the maternal decidua and come into direct contact with maternal blood and tissues (3). During this invasive process, trophoblast cells transform the uterine arteries into large canals that funnel maternal blood toward the implantation site (4–6). Spiral artery remodeling is initiated early after implantation and is critical for the establishment of a fully functional placental nutrient and gas exchange unit throughout further development.

How precisely the conceptus evades immune rejection in this context remains elusive (7). An important mechanism may be provided by the distinctive MHC antigen expression profile on the surface of trophoblast. In humans, invasive extravillous trophoblast cells lack the highly polymorphic classical MHC class I (HLA-A and -B) and class II antigens but instead express a unique combination of classical HLA-C and nonclassical HLA-G and HLA-E molecules (8–10). Because nonclassical MHC class I molecules are invariant and HLA-G is expressed in the thymus, these antigens do not elicit prominent maternal immune responses (11, 12). Only HLA-C shows any appreciable polymorphism, and therefore the fetus will differ from the mother depending on the HLA-C allele contributed by the father. HLA-C is the dominant ligand for killer Ig-like receptors (KIR) expressed on natural killer (NK) cells (13). Indeed, uterine NK (uNK) cells are the most likely maternal cell type to interact with trophoblast antigens in the decidua basalis because of their sheer abundance: they constitute 70% of all maternal leukocytes in the placental bed (14). uNK cells differ from peripheral NK cells in that they have a reduced lytic activity and a distinct surface receptor repertoire (14–17). uNK cells support neovascularization of the decidua by producing proangiogenic and endothelial mitogenic stimulants and contribute to arterial transformation by initiating the loss of the arterial media (5, 14, 18, 19). In uNK cell-deficient mice the arteries do not undergo the dilation that is normally observed during pregnancy, and the resulting decrease in maternal blood supply may be associated with small placental size and embryonic lethality (20, 21). Thus, normal progression of pregnancy seems to be influenced by the functional activity of uNK cells, which in turn may be regulated by the paternal MHC expression on trophoblast through direct or indirect interactions.

The importance of trophoblast–uNK cell interactions has been reinforced by the finding that certain combinations of maternal KIRs and fetal HLA-C seem unfavorable to trophoblast cell invasion and are associated with pregnancy disorders (22, 23). These disorders include preeclampsia and fetal growth restriction and are all due to defective placentation and inadequate arterial transformation. Thus, the immunological interplay between MHC expressed by fetal trophoblast and maternal uNK cells is critical for normal remodeling of decidual arteries.

How these maternal–fetal immunological interactions dictate the outcome of pregnancy remains unknown. The mouse can provide a particularly useful tool for the detailed investigation of this mechanism, both because strains exist that are homozygous for specific MHC haplotypes and because it is possible to derive and maintain trophoblast stem (TS) cells in vitro that can differentiate into all trophoblast cell types (24). However, a key question is whether mouse trophoblast expresses MHC class I antigens that could functionally interact with uNK cell receptors. Several studies have suggested the presence of H2 molecules, which represent the main group of MHC class I antigens in the

Author contributions: Z.M., H.Y., R.A., A.M., F.C., and M.H. designed research; Z.M., H.Y., R.A., S.B., S.J.R., L.G., and M.H. performed research; Z.M., H.Y., R.A., S.B., S.J.R., L.G., A.M., F.C., and M.H. analyzed data; and F.C. and M.H. wrote the paper.

The authors declare no conflict of interest.

This article is a PNAS Direct Submission.

[1]Present address: Department of Genetics and Animal Breeding, University of Life Sciences, 60-637 Poznan, Poland.

[2]F.C. and M.H. contributed equally to this work.

[3]To whom correspondence should be addressed. E-mail: myriam.hemberger@bbsrc.ac.uk.

This article contains supporting information online at www.pnas.org/lookup/suppl/doi:10.1073/pnas.1005342108/-/DCSupplemental.

mouse, either at the RNA level or by antisera binding (25–29). What is still unknown is which H2 loci are expressed as proteins, whether they are displayed at the cell surface, and on which trophoblast subsets they are found. Of particular importance is the nature of MHC expression on trophoblast giant cells as they form the boundaries of the implantation site, invade into the mesometrial decidua, and contribute to arterial remodeling. To gain better insights into the immunological competence of mouse trophoblast, we here characterized systematically its MHC antigenic profile and investigated the impact of an antigenic dissimilarity between mother and fetus on trophoblast invasion, uterine vascular remodeling, and fetal and placental growth rates. Our data provide insight into the importance of immunological interactions at the maternal–fetal interface for reproductive success and demonstrate how the immunological paradox has been redirected to the benefit of the fetus during the evolution of viviparity.

Results

MHC Class I mRNA Expression in Mouse Trophoblast. Expression of the two classical MHC class I molecules *H2-K* and *H2-D* on mouse trophoblast was first assessed by haplotype-specific RT-PCR on gestational day (E) 8.5 ectoplacental cone samples dissected from crosses between the C57BL/6 (B6; *b* haplotype) and BALB/c (*d* haplotype) strains. In all cases, we detected expression of both *H2-K* and *H2-D* genes (Fig. 1*A*). The intercross-derived samples served to prove expression of the paternal MHC allele. Thus, the *H2-K*^{b} and *H2-D*^{b} products in the BALB/c × B6 cross (mother is always named first) stemmed from the *b* allele of the B6 father, and likewise the *H2-K*^{d} and *H2-D*^{d} bands were derived from the paternal *d* allele in the B6 × BALB/c cross. Haplotype specificity of the PCRs was proved by the absence of a product with the strain-foreign haplotype-specific primers in the inbred crosses (Fig. 1*A*). Representative PCR products were sequenced to confirm their identity. Trophoblast-specific expression of H2-K and H2-D was also recapitulated in TS cells derived from the B6 strain (Fig. S1).

Although both antigens were detected, quantitative RT-PCR (qRT-PCR) revealed that *H2-K*^{b} was the predominant MHC molecule expressed by B6 mouse trophoblast, with 18-fold higher transcript levels in TS cells than *H2-D*^{b} (Fig. 1*B*). To determine whether expression levels differed between stem cells and differentiated trophoblast cell types, TS cells were cultured in the absence of FGF4 and feeder cell-conditioned medium for 6–8 d, which induces down-regulation of stem cell-expressed genes such as *Cdx2* and differentiation mainly into trophoblast giant cells (24, 30). Intriguingly, *H2-K*^{b} and *H2-D*^{b} mRNA expression was strikingly higher in giant cells than in undifferentiated TS cells (15-fold for *H2-K*^{b} and fourfold for *H2-D*^{b}; Fig. 1*B*). Despite this overall increase, *H2-K*^{b} was still the predominant MHC class I antigen in giant cells (i.e., the trophoblast cell type that comes into direct contact with maternal tissues).

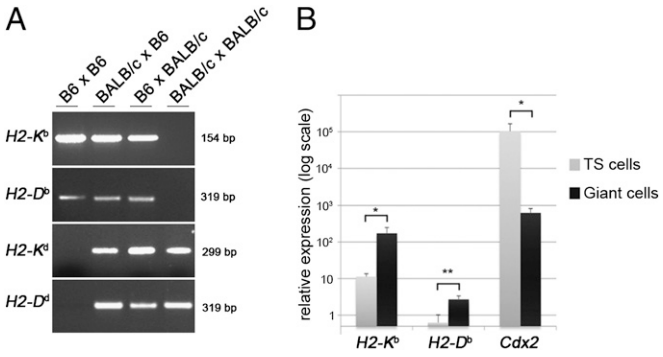

Fig. 1. MHC class I expression in mouse trophoblast. (*A*) Haplotype-specific RT-PCR analysis for MHC class I molecules *H2-D* and *H2-K* in ectoplacental cone trophoblast dissected from mouse E8.5 implantation sites of syngeneic and allogeneic matings. Haplotype-specific primers were used to distinguish the C57BL/6 ("*b*" haplotype) and BALB/c ("*d*" haplotype) alleles. Note that the *H2-K*^{b} and *H2-D*^{b}-specific bands in the BALB/c × B6 cross are derived from expression of the paternal B6 allele, and conversely the *H2-K*^{d} and *H2-D*^{d} bands in the B6 × BALB/c mating originate from the paternal BALB/c allele. (*B*) qRT-PCR analysis of *H2-K*^{b} and *H2-D*^{b} in TS cells of C57BL/6 genotype and giant cells differentiated from them. The relative expression levels of both antigens were significantly higher in giant cells compared with TS cells. *$P < 0.05$; **$P < 0.005$. *Cdx2* is a TS cell marker that is down-regulated upon differentiation and was used as a control.

MHC Class I Protein on the Surface of Mouse Trophoblast Giant Cells. Next we determined whether transcript levels of these classical MHC class I antigens correlated with their presence on the surface of trophoblast cells. Three different methods (FACS, immunoprecipitation, and immunofluorescence staining) were used to study surface MHC expression. Compared with IgG control, the anti–H2-K monoclonal antibody unambiguously stained the surface of trophoblast cells (Fig. 2 and Figs. S2 and S3). By contrast, H2-D was only detectable at very low levels by FACS, with variable results presumably due to slightly varying

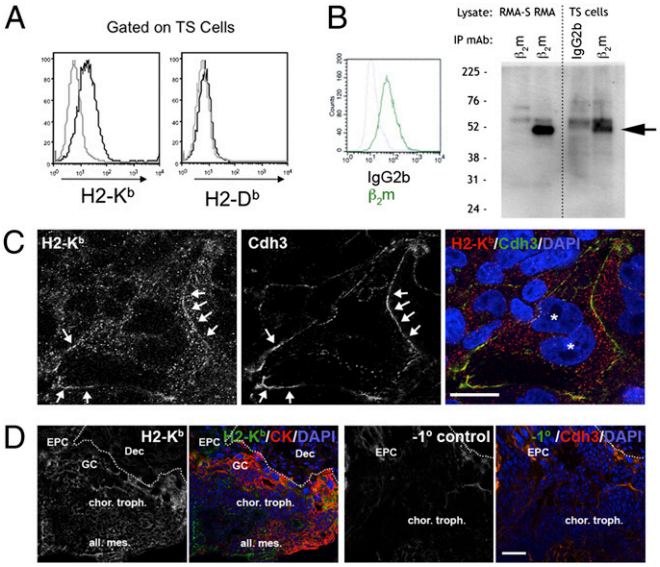

Fig. 2. H2-K^{b} and H2-D^{b} MHC class I antigens on the surface of TS cells. (*A*) B6 TS cells were analyzed by flow cytometry. Expression of H2 was assessed using a gate that included stem cells and slightly larger, partially differentiated trophoblast cell populations. H2-K^{b} and H2-D^{b} staining (black line) overlaid with isotype control (gray line) stain on TS cells. (*B*) TS cells differentiated for 1 d were stained for anti-β_2m and analyzed by flow cytometry. Immunoprecipitation with anti-β_2m and Western blotting for surface proteins labeled by biotinylation shows that the antigen recognized by anti-β_2m on trophoblast is the same size as H2 molecules of the control RMA, but not TAP2-deficient RMA-S, cell lines. (*C*) Immunofluorescent staining of partially differentiated B6 TS cells indicating the presence of the H2-K^{b} antigen on the surface of giant cells. Cdh3 was used as a cell-surface marker. White asterisks demarcate a bipartite giant cell nucleus (DAPI staining). White arrows indicate colocalization of H-2K^{b} (red) and Cdh3 (green) on the cell membrane. (*D*) H2-K^{b} staining on E8.5 implantation sites of BALB/c × B6 crosses where paternal H2-K^{b} is expressed on fetal-derived cells but is absent from the maternal decidua. Trophoblast was marked by pan-cytokeratin (CK) or Cdh3 staining. Surface H2-K^{b} is observed on chorionic trophoblast (chor. troph.) and stronger on giant cells (GC) at the interface to the maternal decidua (Dec). Note that background staining is evident in intercellular spaces around some ectoplacental cone (EPC) cells but is clearly distinct from specific H2-K^{b} signals. All. Mes. = allantoic mesoderm. (Scale bars, 25 μm in *C*, 50 μm in *D*.)

differentiation states of the TS cell cultures (Fig. 2*A* and Fig. S2). Locus and allele reactivity of the monoclonal antibodies used is well established (31), and we also confirmed specificity using splenic controls (Fig. S2). Immunoprecipitation of trophoblast surface proteins using a monoclonal antibody to β2-microglobulin (β_2m), associated with all MHC class I molecules, confirmed that the MHC heavy chain on mouse trophoblast was the same molecular weight (45 kDa) as for classical H2 antigens of the RMA control cell line (Fig. 2*B*). No lower-molecular-weight bands suggestive of nonclassical MHC molecules were detected (32). In line with the RT-PCR data, we observed a clear increase in H2-K^b and β_2m staining upon TS cell differentiation (Fig. S4). To resolve the cell type-specific expression pattern, we stained partially differentiated B6 TS cells, ectoplacental cone explants of B6 conceptuses, and E8.5 (BALB/c × B6) implantation sites for H2-K^b by immunofluorescence and assessed them by confocal microscopy. In all these contexts, clear and specific H2-K^b staining was detected both in the cytoplasm and on the cell membrane, as revealed by costaining with the trophoblast surface marker Cdh3 (Fig. 2*C* and Fig. S3). Importantly, the strongest H2-K^b staining was always confined to giant cells: those differentiated from TS cells in vitro (Fig. 2*C*), giant cells in ectoplacental cone explants (Fig. S3*B*), and those at the interface with the decidua in implantation sites in vivo (Fig. 2*D*).

In addition to the two classical MHC class I loci (K and D), more than 20 nonclassical class I genes have been identified in the B6 genome that may be particularly important on trophoblast (32). Transcripts for many of these nonclassical class I genes have been detected in crude placental extracts (32). Classical and nonclassical H2 genes of B6 mice show significant homology, averaging 92% nucleotide sequence identity in the conserved α3 domain (32). To identify whether any nonclassical H2 genes are expressed, we performed RT-PCR with degenerate primers amplifying H2-K, H2-D, and each of the M, Q, and T families of nonclassical H2 genes encoded in B6 mice. This analysis revealed almost exclusively H2-K and H2-D molecules. Only few clones represented the nonclassical T22 transcript, but surface expression was not detected (Fig. S5). Thus, the predominant MHC class I molecule on mouse trophoblast is the classical H2-K and possibly some, albeit considerably less, H2-D on giant cells, but negligible nonclassical MHCs.

The cell surface localization of H2-K would allow for a functional interaction with maternal immune cells, in particular with the cognate Ly49 receptors on the surface of uNK cells (15). Indeed, we found that paternal H2-K^b affected the maternal uNK cell repertoire, because more Ly49C-positive uNK cells were detected in the decidua of ($d \times b$) allogeneic crosses compared with ($d \times d$) syngeneic controls (Fig. S6). This result indicates that the maternal uNK cell receptor repertoire may adapt to the paternal H2-K^b expressed by trophoblast.

Physical Interactions Between Trophoblast and uNK Cells. Surface expression of MHC antigens and their functional effect on uNK cells raised the question of whether trophoblast cells physically interact with uNK cells to influence their activity. Previous studies on E13.5 placentas suggested that uNK cells are separated from the farthest distal trophoblast cells by a considerable distance (5). Because the remodeling of uterine arteries is initiated much earlier during the phase of trophoblast giant cell invasion, we analyzed midsagittal sections of E8.5 conceptuses for the relative distribution of uNK and trophoblast cells, detected by staining with *Dolichus biflores* agglutinin (DBA) and pan-cytokeratin, respectively (5, 33). At this stage it was obvious that trophoblast cells in the mesometrial decidua were surrounded by large numbers of uNK cells, some of which had infiltrated the ectoplacental cone (Fig. 3 *A* and *B*). Confocal microscopy confirmed that uNK cells are frequently found directly juxtaposed to trophoblast in early postimplantation conceptuses (Fig. 3*C*).

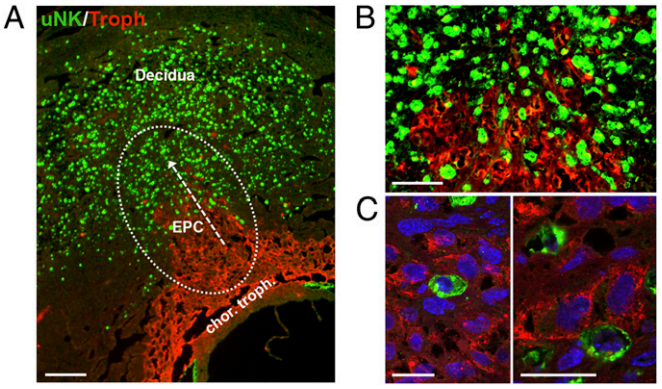

Fig. 3. Physical interaction of trophoblasts and uNK cells in the mouse implantation site. (*A*) Sagittal sections of E8.5 mouse implantation sites stained for pan-cytokeratin (red) as a trophoblast marker and DBA as a uNK cell marker (green). The ectoplacental cone (EPC) and direction of trophoblast invasion is indicated. chor. troph. = chorionic trophoblast. (*B*) Magnified area from *A* showing the close juxtaposition of trophoblast and uNK cells in the ectoplacental cone region. (*C*) Confocal microscopy analysis visualizes uNK cells in direct contact with trophoblast cells, demonstrating the physical possibility of receptor–ligand mediated interactions. (Scale bars, 200 μm in *A*, 100 μm in *B*; 50 μm in *C*.)

Thus, uNK cells come into intimate physical contact with trophoblast cells for direct MHC–uNK cell receptor interactions.

Functional Consequences of Antigenic Dissimilarity Between Mother and Fetus. Transformation of the uterine vasculature is a unique process that depends on uNK cells as well as invasive trophoblast. To test whether the interactions between both cell types influence decidual artery remodeling in vivo, we analyzed serial transverse sections of E8.5 B6 and BALB/c conceptuses and their reciprocal intercrosses throughout the thickness of the uterine wall. By determining the distance between the base of the ectoplacental cone and the deepest invading giant cells, we found that maternal–fetal MHC combinations did not affect the depth of trophobast invasion (Fig. S7*A*). By contrast, dramatic differences in the extent of decidual artery dilation were observed that depended on the direction of the cross. Staining the sections containing the most distally invading giant cells with an endothelial cell marker (von Willebrand factor) allowed us to measure the diameter of blood vessels in corresponding decidual regions in the four different crosses. Strikingly, decidual artery diameters of BALB/c × B6 conceptuses were approximately twice as large as those of the inbred strains as well as the reciprocal B6 × BALB/c cross (Fig. 4 *A* and *B*). Thus, the B6 genotype of the father in the allogeneic BALB/c × B6 cross has a profound effect on uterine vascularization compared with the syngeneic BALB/c × BALB/c mating (i.e., same maternal genotype). The direction of the cross made a significant difference because the arterial diameters in the B6 × BALB/c intercross were much less affected than in the BALB/c × B6 cross. This indicated that the effect is specific to particular strain combinations and is therefore not simply the result of heterosis.

Paternal MHC Affects Decidual Vascularization, as Well as Placental and Fetal Growth. We hypothesized that the strain-specific effect on decidual vessel dilation was due to maternal BALB/c uNK cells interacting with paternal H-2K^b on trophoblast. To test this hypothesis, we narrowed down the genetic variability between the parents by using the congenic BALB.B strain that carries the *b* haplotype at the H2 locus on a BALB/c genetic background (34). Because of the dramatic effect of a B6 father (carrying the *b* haplotype) crossed to a BALB/c female on decidual vessels, we concentrated on the same combination of haplotypes in the

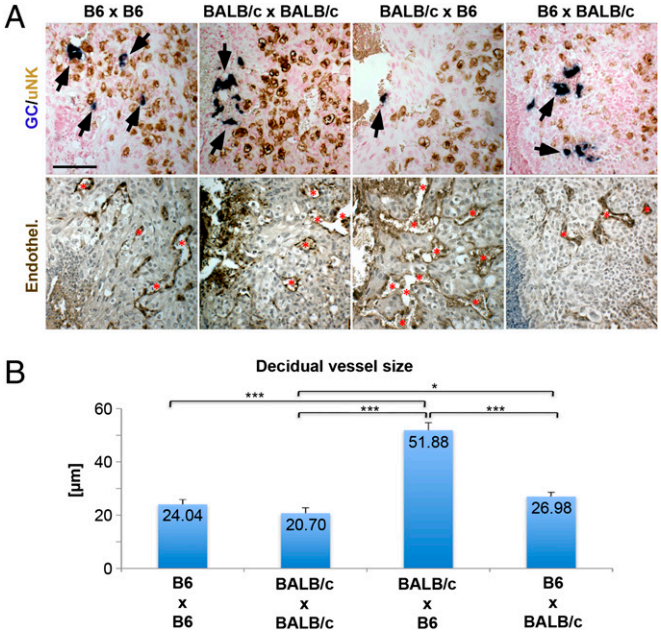

Fig. 4. Antigenic dissimilarity between mother and fetus affects decidual blood vessel size. (*A*) Serial transverse sections of E8.5 implantation sites from syngeneic and allogeneic crosses between B6 and BALB/c were used for in situ hybridization with the invasive trophoblast giant cell marker *Prl4a1*, also known as *Prlpa* (blue) followed by DBA immunostaining as a uNK cell marker (brown) and nuclear counterstaining (red). *Prlpa* staining identified the section with the farthest invading giant cells (arrows). The adjacent section was stained for endothelial cells (von Willebrand factor) and analyzed for decidual vessel diameter. Red asterisks demarcate blood vessels. (Scale bar, 100 µm.) (*B*) Vessel diameter analysis reveals that combination of a BALB/c mother and B6 father results in a particular increase in decidual blood vessel size. This analysis is based on four conceptuses per mating from two independent litters each (i.e., 2 + 2 per mating). Although both allogeneic crosses result in a genetic F1 generation, the two reciprocal matings are not equal. $*P < 0.05$; $***P < 0.0005$.

congenic matings by crossing BALB/c females to BALB.B males. Despite some variability between conceptuses (Fig. S7*B*), vessels were on average 1.5-fold wider upon introduction of an allogeneic $H2^b$ haplotype than in the syngeneic control (Fig. 5 *A* and *B*). Thus, remarkably, approximately 50% of the (BALB/c × B6) F1 phenotype is recapitulated in the BALB/c × BALB.B cross and is therefore attributable to the introduction of foreign paternal MHC-linked genes.

Appropriate dilation of the uterine vasculature results from arterial remodeling and loss of vasoconstrictive control, which are key adjustments in early pregnancy to ensure a sufficient blood and nutrient supply for normal fetal growth and development. To determine whether the allogeneic MHC could indeed have a long-lasting effect on developmental outcome, we assessed the weights of placentas and fetuses at E18.5 of BALB/c / BALB.B F1 (semi)allogeneic and BALB/c / BALB/c syngeneic conceptuses (Fig. 5 *C*–*E*). These conceptuses were derived from two different sets of matings, from BALB/c × BALB/c and BALB/c × BALB.B, as well as from BALB/c × (BALB/c × BALB.B) F1 in which syn- and allogeneic conceptuses develop within the same mother. To achieve the most powerful statistical analysis, we pooled all weight data of BALB/c / BALB/c syngeneic and BALB/c / BALB.B allogeneic fetuses and placentas from both experimental sets. BALB/c / BALB.B fetuses allogeneic at the H2 locus were larger than syngeneic controls ($P = 0.006$), and this effect was not influenced by litter size ($P = 0.228$) (Fig. 5*C*). Allogeneic BALB/c / BALB.B placentas were also larger, but this effect was dependent on litter size: the bigger the litter, the smaller the difference ($P = 0.01$) (Fig. 5*D*). These data imply that allogeneic placentas may be more efficient in supporting fetal growth in larger litters, in which maternal resources are more restricted. The increased fetal/placental weight ratios of BALB/c / BALB.B conceptuses in larger litters do indeed demonstrate an augmented placental efficiency (Fig. 5*E*), suggesting a growth-enhancing effect of the increased maternal blood supply through larger spiral arteries on these allogeneic conceptuses.

Discussion

Our ignorance about which MHC molecules are expressed on the surface of murine trophoblast has held back research in the field of reproductive immunology. Using a variety of approaches, we here show that mouse trophoblast is immunologically competent and expresses the classical MHC class I molecule H2-K on the cell surface. Taking advantage of intercrosses between mouse strains with defined H2 haplotypes, we further demonstrate presence of the paternal H2-K allele on trophoblast giant cells. These results correlate with previous reports of the detection of MHC transcripts in preimplantation embryos and trophoblast samples from E7.5 onward (27, 28) and presence of paternal H2-K antigens on early trophoblast and on the sinusoidal face of mouse labyrinthine trophoblast cells in the late-gestation placenta (25, 26, 35). In contrast to the typical coexpression of H2-K and H2-D on the surface of virtually all nucleated cells, however, we find that mouse trophoblast expresses only one predominant classical polymorphic MHC molecule, H2-K. This situation resembles that of human trophoblast that expresses only HLA-C but lacks the polymorphic HLA-A and HLA-B antigens. An unusual trophoblast MHC class I repertoire is thus conserved between both species and may be essential for trophoblast function at the maternal–fetal interface.

Interestingly, however, unlike human trophoblast that characteristically expresses HLA-G and -E, nonclassical MHC class I antigens are not a prominent feature on B6 mouse trophoblast. Thus, we did not detect mRNA and/or surface expression of the nonclassical M, Q, or T family genes, and immunoprecipitation using a monoclonal antibody to β_2m only revealed heavy chains with a molecular weight of classical MHC molecules. This lack of nonclassical H2 molecules on murine trophoblast corresponds with the absence of their cognate receptors (CD94 and NKG2ACE) on the DBA^+ uNK cells both in the B6 and BALB/c strains (15). Thus, nonclassical MHC class I molecules are not a prerequisite for trophoblast function in species with hemochorial placentation.

We have also determined the anatomical location of MHC antigens in murine trophoblast subsets. Early studies suggested the absence of MHC class I antigens on giant cells of the ectoplacental cone, but this view was revised by experiments using in situ hybridization and immunogold labeling techniques (25, 28, 35, 36). We here used TS cells, ectoplacental cone explants, and implantation sites to unequivocally resolve the cell type-specific distribution of H2 expression. All of our approaches perfectly correlate in demonstrating that H2-K is more strongly expressed on giant cells than in undifferentiated trophoblast. We also show that giant cells frequently come into intimate contact with uNK cells in E8.5 implantation sites. Thus, trophoblast cells that are in direct contact with maternal tissues express polymorphic MHC molecules of maternal and paternal origin on their surface, allowing them to functionally interact with surrounding immune cells.

Maternal uNK cells are the main candidate at the site of placentation to interact with fetal trophoblast. The receptor repertoire of uNK cells is unique and, as we show here, can be influenced by the presence of trophoblast. $H2\text{-}K^b$ is the cognate ligand for the NK cell inhibitory receptor Ly49C, and $H2\text{-}K^b$–Ly49C interactions impact on the functional maturation of peripheral NK cells (37). Paternal $H2\text{-}K^b$ seems to interact with the inhibitory Ly49C receptor expressed on the BALB/c maternal uNK cells in the strain combination we have used. Indeed, the

DEVELOPMENTAL BIOLOGY

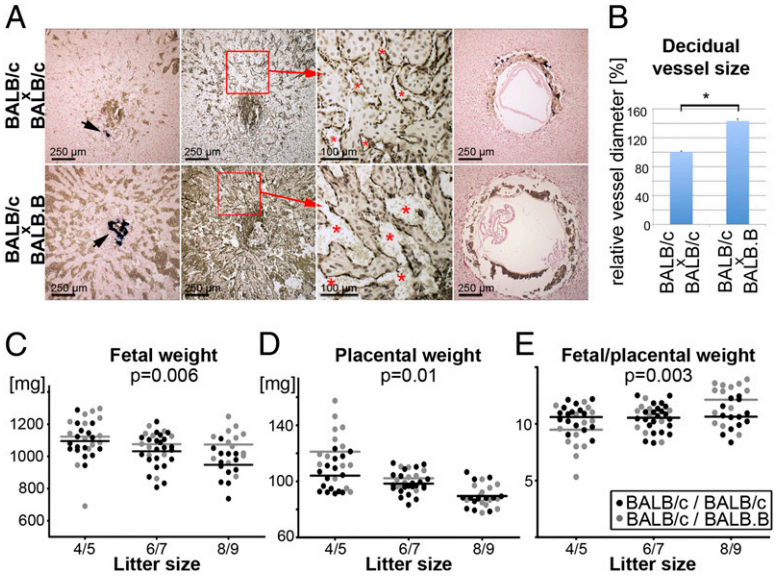

Fig. 5. Paternal MHC-modulated decidual vascularization affects placental and fetal size. (*A*) In situ hybridization against *Prlpa* to detect the farthest invading giant cells (arrows, *Left*) and endothelial cell staining on the adjacent section of E8.5 syngeneic (BALB/c × BALB/c) and allogeneic (BALB/c × BALB.B) conceptuses. The boxed area is shown in magnification. Red asterisks demarcate blood vessels. The right-most panels show cross-sections through the embryonic region to confirm normal development. Note that the embryo of the BALB/c × BALB.B mating with the highly vascularized decidua is larger. Size of magnification bars is given. (*B*) Decidual blood vessel size is increased by 40–50% when the paternal $H2^b$ haplotype is introduced, recapitulating the effect in the hybrid (BALB/c × B6) F1 situation. Values are from 11 BALB/c × BALB/c and 6 BALB/c × BALB.B conceptuses, assembled from three independent matings each (i.e., 4 + 4 + 3 conceptuses for BALB/c × BALB/c and 2 + 2 + 2 conceptuses for BALB/c × BALB.B). Two-way ANOVA performed on a random selection of six conceptuses each demonstrated that the difference between the crosses is significant. $*P = 0.041$. (*C*) Fetal wet weights at E18.5 of syngeneic BALB/c / BALB/c ($n = 63$) and allogeneic BALB/c / BALB.B ($n = 40$) conceptuses derived from matings of BALB/c × BALB/c ($n = 6$) and BALB/c × BALB.B ($n = 4$), as well as BALB/c × (BALB/c × BALB.B) F1 ($n = 8$) of comparable litter sizes. Two-way analysis of variance was performed taking into account genotype and litter size. BALB/c/BALB.B allogeneic fetuses are significantly heavier ($P = 0.006$), and this difference does not depend on litter size. (*D*) Placental weights of the corresponding fetuses shown in *C*. Placentas of allogeneic conceptuses are also heavier than syngeneic controls, but this difference is dependent upon litter size ($P = 0.01$): the bigger the litter, the smaller the difference. (*E*) Fetal/placental weight ratios of conceptuses in *C* and *D*. Because allogeneic fetuses in large litters are significantly heavier, whereas the placental weight difference is less pronounced, the allogeneic placenta is more efficient in supporting fetal growth per gram placenta. $P = 0.003$.

frequency of $Ly49C^+$ uNK cells was greater in the presence of paternal $H2\text{-}K^b$, providing in vivo evidence of an adaptation of uNK cell receptors to paternal MHC. Investigations on the potential contribution of paternal H2 antigens to Ly49-mediated uNK cell education will shed light on the mechanisms of interaction between uNK cells and paternal MHC class I molecules. In addition to H2-K and Ly49 receptors, other types of interactions could occur between trophoblast and uNK cells. Indeed, we found that mouse trophoblast expresses transcripts for E-cadherin (*Cdh1*), the ligand for KLRG1, which is highly expressed on uNK cells (15), and *Gas6* as well as *Pros1* transcripts, which are implicated in the regulation of NK cell differentiation (Fig. S8) (38).

Because both trophoblast and uNK cells contribute to the transformation of decidual arteries, an intriguing functional consequence of their interaction may be to regulate the progression of this remodeling process. Indeed, we show here that the allogeneic paternal H2-K expressed on fetal trophoblast enhances the dilation state of maternal blood vessels. This in turn correlates with a growth advantage in late gestation, with larger pups and more efficient placentas at term.

Overall our findings in these murine models reveal striking similarities with placentation in humans. We have recently described expression of paternal HLA-C allotypes in the invasive trophoblast cells that are in close proximity to uNK cells at the implantation site. Genetic studies show that variations in maternal and paternal HLA-C groups as well as maternal KIR genotypes influence reproductive success, in particular common and important human pregnancy disorders, such as fetal growth restriction, recurrent miscarriage, and preeclampsia (23). Thus, our findings give great confidence that murine models will provide useful tools to study the importance of immunological crosstalk during placentation. The impact on fetal growth makes this immunological interaction also a key player in fetal programming for developmental origins of adult diseases (39).

Materials and Methods

Mice and TS Cell Lines. Mice of inbred strains BALB/cAnNCrl and C57BL/6J (B6) and their reciprocal intercrosses were used. BALB.B mice were originally generated by backcrossing C57BL/10 mice (carrying the $H2^b$ haplotype) to the BALB/c strain for 13 generations and selecting for the $H2^b$ genotype (34). Cryopreserved BALB.B embryos were a kind gift from the National Institute of Medical Research, London. In all matings, the female is indicated first. Pregnant females from natural matings were dissected at the gestational age indicated, counting the morning of the vaginal plug as E0.5. Conceptuses of BALB/c × (BALB/c × BALB.B) F1 litters were genotyped by FACS on fetal liver cells using monoclonal antibodies against $H2\text{-}K^b$ and $H2K^d$, as well as by H2-K haplotype-specific PCR. TS cell lines were derived from the C57BL/6J strain and were a kind gift of Dr. A Erlebacher (New York University School of Medicine).

RT-PCR and qRT-PCR. Total RNA was extracted using TRIzol reagent (Invitrogen); 2 µg was used for cDNA synthesis followed by qPCR. Each sample was analyzed in triplicate; each analyzed group contained 6–14 independent samples. Normalization was performed against Dynein. All primer pairs were designed to span introns (Table S1). PCR products were sequence-verified. For degenerate PCRs, four reactions were used, one each for the Q and M families of nonclassical H2 genes and two for the T family (Table S2). Five nonclassical genes would not be amplified: T13, T15, and T24 differ substantially in size from the H2 molecule immunoprecipitated by the anti-β_2m antibody, and M1 and M10 are well established components of vomeronasal pheromone receptors.

Immunohistochemistry/Immunofluorescence. TS cells and ectoplacental cone explants were cultured on coverslips, fixed with 4% paraformaldehyde, and permeabilized with 0.1% Triton X-100 in PBS or postfixed with acetone. Antibodies used were purified anti-mouse H2-K^b (AF 6-88.5, BD Biosciences, Pharmingen) at 1:100, and anti Cdh3 (MS-1741-S0, NeoMarkers) at 1:200. H2-K^b staining on implantation sites was on frozen sections as above. For trophoblast-uNK localization studies, sagittal paraffin sections of E8.5 conceptuses were stained with anti–pan-cytokeratin (Z0622, DAKO) at 1:100, followed by staining with FITC-conjugated DBA (L9142, Sigma). Counterstaining was performed with DAPI. Epifluorescent images were taken on an Olympus Bx41 microscope and confocal images on a Zeiss 510 Meta microscope.

FACS Analysis. B6 TS cells were harvested using 2 mM EDTA and used in parallel to cell suspensions from spleens of B6 (positive control) and BALB/c (negative control) mice. Antibodies used were phycoerythrin (PE)-labeled H2-K^b (clone AF 6-88.5, BD Biosciences, Pharmingen), PE-labeled H2-D^b (clone KH95, BD Biosciences, Pharmingen), and isotype controls. Anti-β_2m antibody (clone S19.8, BD Biosciences) was detected with polyclonal PE-conjugated antibody to murine IgG (Sigma-Aldrich). Cells were analyzed on a BD Biosciences LSRII flow cytometer. Analyses of data were performed using FloJo (Tree Star) software.

Immunoprecipitation. TS cells were biotinylated with 0.2 mg/mL EZ-Link Sulfo-NHS-LC-Biotin (Pierce) for 20 min at 4 °C. Unconjugated reagent was quenched with 10 mM glycine, and cells were lysed in a fresh preparation of 20 mM Tris (pH 7.4), 140 mM NaCl, 1 mM EGTA, 1% Triton, 10% glycerol, 50 mM iodoacetamide, and protease inhibitor mixture (Roche). Lysates were precleared with protein G-Sepharose beads (Amersham Biosciences) before immunoprecipitation with anti-β_2m antibody or isotype control precoated protein G-Sepharose beads. Immunoprecipitated complexes were washed with lysis buffer containing 3 mM SDS before bound proteins were eluted with NuPAGE LDS Sample Buffer (Invitrogen), denatured by heating to 95 °C, resolved on reducing NuPAGE Bis-Tris 10% gels (Invitrogen), electroblotted, and visualized with streptavidin-HRP detected by ECL Plus (Amersham Biosciences). Parental RMA mouse lymphoma cells (H2^b) and TAP2-deficient RMA-S mouse lymphoma cells were used as control in immunoprecipitation.

Histology and in Situ Hybridization. Whole uterine horns of pregnant females were dissected, the main uterine artery tied to minimize bleeding, fixed overnight in 4% paraformaldehyde, and processed for paraffin histology. Conceptuses were embedded in transverse orientation and serially sectioned at 7 μm. In situ hybridizations were performed with digoxigenin-labeled riboprobes according to a standard protocol. The *Prl4a1* probe was a kind gift of Dr. M. Soares (University of Kansas Medical Center, Kansas City, KS). Where indicated, sections were subsequently stained with HRP-conjugated DBA lectin (Sigma). Counterstaining was performed with hematoxylin or nuclear fast red.

Vessel Diameter Measurements. To minimize variations in the level of dehydration, all conceptuses that were directly compared were processed in parallel for paraffin histology, were embedded in the same block, and thus mounted and stained on the same slide. Sections adjacent to those with the deepest invading giant cells were stained for von Willebrand factor (A0082, DAKO) at 1:100. The longest and widest distances (at orthogonal angles) were measured for each vessel using ImageJ software. At least four independent conceptuses per cross were analyzed.

ACKNOWLEDGMENTS. We thank Dr. Anne Segonds-Pichon for expert statistical analyses of our data and Prof. Elizabeth Simpson for critically reading the manuscript. This work was supported by a Biotechnology and Biological Sciences Research Council (BBSRC) Core Support grant from the Babraham Institute (to F.C. and M.H.), the Centre for Trophoblast Research, Cambridge, the Wellcome Trust, the BBSRC, and the Medical Research Council United Kingdom.

1. Parham P (1996) Immunology: Keeping mother at bay. *Curr Biol* 6:638–641.
2. Erlebacher A (2001) Why isn't the fetus rejected? *Curr Opin Immunol* 13:590–593.
3. Benirschke K (1983) Placentation. *J Exp Zool* 228:385–389.
4. Pijnenborg R, Vercruysse L, Hanssens M (2006) The uterine spiral arteries in human pregnancy: Facts and controversies. *Placenta* 27:939–958.
5. Adamson SL, et al. (2002) Interactions between trophoblast cells and the maternal and fetal circulation in the mouse placenta. *Dev Biol* 250:358–373.
6. Hemberger M, Nozaki T, Masutani M, Cross JC (2003) Differential expression of angiogenic and vasodilatory factors by invasive trophoblast giant cells depending on depth of invasion. *Dev Dyn* 227:185–191.
7. Medawar PB (1953) Some immunological and endocrinological problems raised by evolution of viviparity in vertebrates. *Symp Soc Exp Biol* 7:320–328.
8. Apps R, et al. (2009) Human leucocyte antigen (HLA) expression of primary trophoblast cells and placental cell lines, determined using single antigen beads to characterize allotype specificities of anti-HLA antibodies. *Immunology* 127:26–39.
9. Kovats S, et al. (1990) A class I antigen, HLA-G, expressed in human trophoblasts. *Science* 248:220–223.
10. Wei XH, Orr HT (1990) Differential expression of HLA-E, HLA-F, and HLA-G transcripts in human tissue. *Hum Immunol* 29:131–142.
11. Crisa L, McMaster MT, Ishii JK, Fisher SJ, Salomon DR (1997) Identification of a thymic epithelial cell subset sharing expression of the class Ib HLA-G molecule with fetal trophoblasts. *J Exp Med* 186:289–298.
12. Apps R, Gardner L, Moffett A (2008) A critical look at HLA-G. *Trends Immunol* 29: 313–321.
13. Moffett A, Hiby SE (2007) How does the maternal immune system contribute to the development of pre-eclampsia? *Placenta* 28(Suppl A):S51–S56.
14. Moffett A, Loke C (2006) Immunology of placentation in eutherian mammals. *Nat Rev Immunol* 6:584–594.
15. Yadi H, et al. (2008) Unique receptor repertoire in mouse uterine NK cells. *J Immunol* 181:6140–6147.
16. Croy BA, et al. (2003) Uterine natural killer cells: Insights into their cellular and molecular biology from mouse modelling. *Reproduction* 126:149–160.
17. Moffett-King A (2002) Natural killer cells and pregnancy. *Nat Rev Immunol* 2:656–663.
18. Leonard S, et al. (2006) Mechanisms regulating immune cell contributions to spiral artery modification—facts and hypotheses—a review. *Placenta* 27(Suppl A):S40–S46.
19. Hanna J, et al. (2006) Decidual NK cells regulate key developmental processes at the human fetal-maternal interface. *Nat Med* 12:1065–1074.
20. Guimond MJ, et al. (1997) Absence of natural killer cells during murine pregnancy is associated with reproductive compromise in TgE26 mice. *Biol Reprod* 56:169–179.
21. Guimond MJ, Wang B, Croy BA (1998) Engraftment of bone marrow from severe combined immunodeficient (SCID) mice reverses the reproductive deficits in natural killer cell-deficient tg epsilon 26 mice. *J Exp Med* 187:217–223.
22. Hiby SE, et al. (2004) Combinations of maternal KIR and fetal HLA-C genes influence the risk of preeclampsia and reproductive success. *J Exp Med* 200:957–965.
23. Hiby SE, et al. (2010) Maternal activating KIRs protect against human reproductive failure mediated by fetal HLA-C2. *J Clin Invest* 120:4102–4110.
24. Tanaka S, Kunath T, Hadjantonakis AK, Nagy A, Rossant J (1998) Promotion of trophoblast stem cell proliferation by FGF4. *Science* 282:2072–2075.
25. Sellens MH, Jenkinson EJ, Billington WD (1978) Major histocompatibility complex and non-major histocompatibility complex antigens on mouse ectoplacental cone and placental trophoblastic cells. *Transplantation* 25:173–179.
26. Chatterjee-Hasrouni S, Lala PK (1982) Localization of paternal H-2K antigens on murine trophoblast cells in vivo. *J Exp Med* 155:1679–1689.
27. Hedley ML, Drake BL, Head JR, Tucker PW, Forman J (1989) Differential expression of the class I MHC genes in the embryo and placenta during midgestational development in the mouse. *J Immunol* 142:4046–4053.
28. Arcellana-Panlilio MY, Schultz GA (1994) Temporal and spatial expression of major histocompatibility complex class I H-2K in the early mouse embryo. *Biol Reprod* 51: 169–183.
29. Erlebacher A, Vencato D, Price KA, Zhang D, Glimcher LH (2007) Constraints in antigen presentation severely restrict T cell recognition of the allogeneic fetus. *J Clin Invest* 117:1399–1411.
30. Hughes M, et al. (2004) The Hand1, Stra13 and Gcm1 transcription factors override FGF signaling to promote terminal differentiation of trophoblast stem cells. *Dev Biol* 271:26–37.
31. Pérarnau B, et al. (1999) Single H2Kb, H2Db and double H2KbDb knockout mice: peripheral CD8+ T cell repertoire and anti-lymphocytic choriomeningitis virus cytolytic responses. *Eur J Immunol* 29:1243–1252.
32. Ohtsuka M, Inoko H, Kulski JK, Yoshimura S (2008) Major histocompatibility complex (Mhc) class Ib gene duplications, organization and expression patterns in mouse strain C57BL/6. *BMC Genomics* 9:178.
33. Paffaro VA, Jr., Bizinotto MC, Joazeiro PP, Yamada AT (2003) Subset classification of mouse uterine natural killer cells by DBA lectin reactivity. *Placenta* 24:479–488.
34. Freedman HA, Lilly F (1975) Properties of cell lines derived from tumors induced by Friend virus in BALB/c and BALB/c-H-2b mice. *J Exp Med* 142:212–223.
35. King NJ, Drake BL, Maxwell LE, Rodger JC (1987) Class I major histocompatibility complex antigen expression on early murine trophoblast and its induction by lymphokines in vitro. II. The role of gamma interferon in the responses of primary and secondary giant cells. *J Reprod Immunol* 12:13–21.
36. Searle RF, Sellens MH, Elson J, Jenkinson EJ, Billington WD (1976) Detection of alloantigens during preimplantation development and early trophoblast differentiation in the mouse by immunoperoxidase labeling. *J Exp Med* 143:348–359.
37. Kim S, et al. (2005) Licensing of natural killer cells by host major histocompatibility complex class I molecules. *Nature* 436:709–713.
38. Caraux A, et al. (2006) Natural killer cell differentiation driven by Tyro3 receptor tyrosine kinases. *Nat Immunol* 7:747–754.
39. Barker DJ (2007) The origins of the developmental origins theory. *J Intern Med* 261: 412–417.